ADVANCED MATERIALS
www.advmat.de

Cable-Type Flexible Lithium Ion Battery Based on Hollow Multi-Helix Electrodes

Yo Han Kwon, Sang-Wook Woo, Hye-Ran Jung, Hyung Kyun Yu, Kitae Kim, Byung Hun Oh, Soonho Ahn, Sang-Young Lee, Seung-Wan Song, Jaephil Cho, Heon-Cheol Shin, and Je Young Kim**

An important focus in product design is the creation of practical and aesthetic devices. In portable electronics, in particular, the limiting factor is often the shape of the battery; indeed, removal of this battery restriction would constitute a disruptive technology that could open up a path for design innovation.[1] However, despite the development of smaller, thinner, and lighter batteries, the existing battery technology is still far from realizing such design flexibility, mainly owing to the fixed shapes, i.e., cylindrical, prismatic, or pouch shape.[2] Hence, there is increasing recognition of the need for a new concept that would permit various product designs previously impossible with traditional technologies.

To this end, flexible batteries are considered a promising solution, owing to their potential to adapt to mechanical stress and accordingly change shape. Furthermore, the progress made in flexible electronics such as roll-up displays and wearable electronics would receive a strong stimulus with the development of bendable/twistable batteries.[3] Several recent studies of energy conversion devices have focused on the development of flexible batteries or supercapacitors[4–7] using soft materials such as polymer electrolytes,[8] nanometer-sized active materials,[9–14] and highly patterned current collectors with high flexibility.[15–17] However, owing to the low energy capacity, the structural limitations of a sheet-like architecture, and/or the lack of desired flexibility,[18] these batteries have not been commercialized as energy sources for versatile wearable electronics that could be in the form of a necklace, bracelet, or textile.

Here, we introduce an unprecedented concept for battery architecture — a cable-type lithium-ion battery—which can achieve extreme levels of mechanical flexibility that have never been achieved before and might indeed provide the breakthrough necessary in flexible electronics. The linear shape and omni-directional flexibility of the cable-type battery render the designer free from conventional constraints, as the battery can be placed anywhere and in any shape. Moreover, instead of mounting the battery inside the device, it could be worn on the wrist, neck, or any other part of the human body, allowing maximum freedom in the device design and a strong boost for the realization of practical wearable electronics.

As illustrated in **Figure 1**, the basic design comprises several electrode (generally anode) strands coiled into a hollow-spiral (helical) core and surrounded by a tubular outer electrode (cathode). With this architecture, the facing area between the anode and cathode is large and, at the same time, the cell capacity and capacity balance between two electrodes can be tuned by adjusting the number of anode strands and the thickness of cathode composite. In the early stages of the study, we tested several designs with a nonhollow core, which all failed to realize predictable cell performance. Moreover, a nonhollow anode proved to have serious problems with penetration of the electrolyte into the essential cell components such as the separator and active materials, as will be discussed later. However, we were able to overcome these drawbacks by devising a unique architecture comprising a skeleton frame surrounding an empty space, that is, a hollow-spiral anode with a multi-helix structure (Figure 1B). This design enables easy wetting of the battery components with the electrolyte and the hollow space allows the device to compensate for any external mechanical distortion while maintaining its structural integrity. In addition, this helical architecture possibly enables the battery to be more flexible, owing to its similarity to a spring-like structure.

The fabrication of the cable battery can be separated into two steps as shown in Figure 1A: i) the formation of the hollow-helix anode and ii) the assembly of other components of the cable battery. First, Ni-Sn active material was electrodeposited on a 150-μm-diameter Cu wire (see Supporting Information, Figures S1 and S2). A twisted bundle was prepared with three

Y. H. Kwon, Dr. S.-W. Woo, H.-R. Jung, Dr. H. K. Yu, Dr. K. Kim, B. H. Oh, Dr. S. Ahn, Dr. J. Y. Kim
Battery R&D, LG Chem, Ltd.
104-1 Moonji-dong, Yuseong-gu, Daejeon, 305-380, Republic of Korea
E-mail: jeykim@lgchem.com
Prof. H.-C. Shin
School of Materials Science and Engineering
Pusan National University
Busan, 609-735, Republic of Korea
E-mail: hcshin@pusan.ac.kr
Prof. S.-Y. Lee
School of Chemical Engineering
Kangwon National University
Chuncheon, Kangwondo, 200-701, Republic of Korea
Prof. S.-W. Song
Graduate School of Green Energy Technology
Department of Fine Chemical Engineering and Applied Chemistry
Chungnam National University
Daejeon, 305-764, Republic of Korea
Prof. J. Cho
School of Energy Engineering and Converging Research Center for Innovative Battery Technologies
Ulsan National Institute of Science & Technology (UNIST)
Ulsan, 689-798, Republic of Korea

DOI: 10.1002/adma.201202196

ADVANCED MATERIALS
www.advmat.de

www.MaterialsViews.com

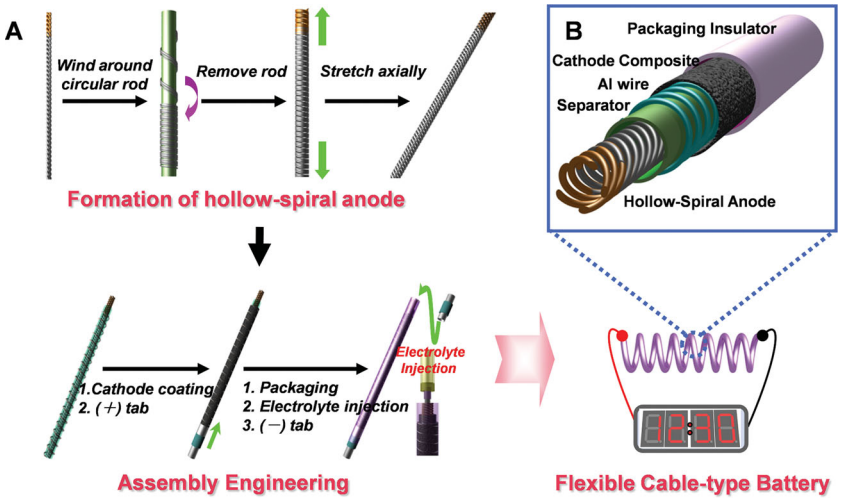

Figure 1. A) Schematic diagram showing fabrication of the cable battery. Ni–Sn-coated Cu wires produced by electroplating were used as the anode. Battery capacity can be simply designed by controlling the number of Ni-Sn-coated wires and the thickness of the cathode composite. Electrolyte was easily injected by inserting a needle into the space inside the hollow-helix anode. B) Schematic illustration of the cable battery with hollow-helix anode having multiple-helix structure. This unique hollow and spring-like structure enables mechanical flexibility and ensures that electrolyte is transported to the electrodes.

strands of Ni-Sn-coated wire by a method similar to that used for producing yarn[19] to achieve a certain degree of stiffness and maintain the hollow frame. Then the hollow-helix anode was fabricated by winding four of the twisted wire bundles around a circular rod (1.5 mm diameter) and pulling axially so that the outer diameter of the anode was about 1.2 mm. After that, we wound a modified poly(ethylene terephthalate) (PET) nonwoven support (separator) and an aluminum wire (cathode current collector) in order around the hollow-helix anode. The slurry for the positive electrode was prepared by mixing $LiCoO_2$, acetylene black, and poly(vinylidene fluoride) binder in a 90:5:5 mass ratio in a solvent of *N*-methyl-2-pyrrolidone (NMP). The anode/separator/Al wire assembly prepared in the previous steps was coated with the slurry by drawing it through a coating bath, followed by drying in a vacuum oven at 120 °C for 10 h. Next, a positive tab consisting of an Al plate and insulating tube was integrated at the end of the positive electrode. Then the electrode assembly was inserted into a heat-shrinkable tube and heated with a heat gun at 130 °C for 1 min to shrink the tube such that the shrunken packaging insulator closely adhered to the outer surface of the electrode assembly. Finally, a liquid organic electrolyte, 1 M lithium hexafluorophosphate ($LiPF_6$) in ethylene carbonate and propylene carbonate (1:1 by volume) containing 3 wt% vinylene carbonate, was injected into the hollow space at the center of the electrode assembly and a negative tab comprising a Ni plate and insulating tube was attached to the end of the negative electrode.

It should be mentioned here why a Ni-Sn anode and modified PET nonwoven separator were selected in this work. Indeed, the Cu wire could have been dip-coated with conventional graphite paste, followed by vacuum-drying to obtain a single anode strand. However, this is not adequate for the hollow-helix anode structure: Severe and repetitive bending inevitably causes loss of electronic contact between the graphite and the conducting additives or Cu wire, leading to poor anode performance. The problem is particularly serious for the inner parts of the spiral, which are structurally unconstrained. In fact, loss of contact starts to appear during the initial step of cell fabrication when the graphite-coated Cu wire anode strands are twisted. This is quite different from what the cathode experiences because the heat-shrinkable tube tightly adheres to the cathode and effectively restrains bending-induced damage.

One possible design option that can guarantee robustness against bending for the anode is to coat Cu wire with a flexible thin film anode material. Sn-based alloys have the most potential for this application and Ni-Sn alloy, in particular, looks promising owing to its acceptable specific capacity and cyclability.[20] The question, however, is how much Ni should be added to the alloy for the present application. With increasing Ni content, the cyclability increases whereas the flexibility reduces as a result of the formation of brittle Ni-Sn intermetallics: thus, cycling and bending stabilities are mutually exclusive in Ni-Sn alloy systems. In this work, we prioritized flexibility over cyclability and accordingly employed ~5 wt% Ni (**Figure 2**).

Next, for the separator membrane, we chose to use a modified PET nonwoven support that has far better thermal stability than commercial polyethylene (PE)[21] because it has to endure relatively high temperatures (>100 °C) during the drying process for the cathode coating and packaging with the heat-shrinkable tubing.

We fabricated a prototype cable battery, as shown in **Figure 3**, and subjected it to various tests to determine its performance. The cross-sectional structure of the cable battery was observed by cutting an epoxy-molded specimen including the assembled cable battery with a cutoff machine (Minitom, Struers). The optical images (Figure 3A and 3B) show the well-constructed morphology of the cable battery, including the hollow-helix anode (outer diameter: 1.2 mm), modified PET nonwoven-support layer (thickness: 50 μm), Al wire (diameter: 200 μm), tubular cathode (thickness: 100–150 μm), and shrunken packaging insulator. As shown in Figure 3C, the hollow-helix anode has a sophisticated helix structure with an empty inner space, which allows facile delivery of electrolyte to the battery components and, in so doing, helps rapid and sustainable electrochemical reactions.

We compared the typical electrochemical properties of a prototype cable battery with a hollow anode with those of a battery with a nonhollow anode, as shown in **Figure 4**. The fabrication procedure for the battery with the nonhollow anode was basically the same as that of the cable battery with the hollow anode, except for the anode preparation and the electrolyte injection: The nonhollow anode was fabricated by just twisting 12 strands of Ni-Sn-coated Cu wire into the shape of a rope or yarn (Figure 4A). After the separator, Al wire, and cathode composite had been introduced, the electrode assembly with the nonhollow anode was saturated with the liquid electrolyte by dipping it into

DOI: 10.1002/adma.201202196

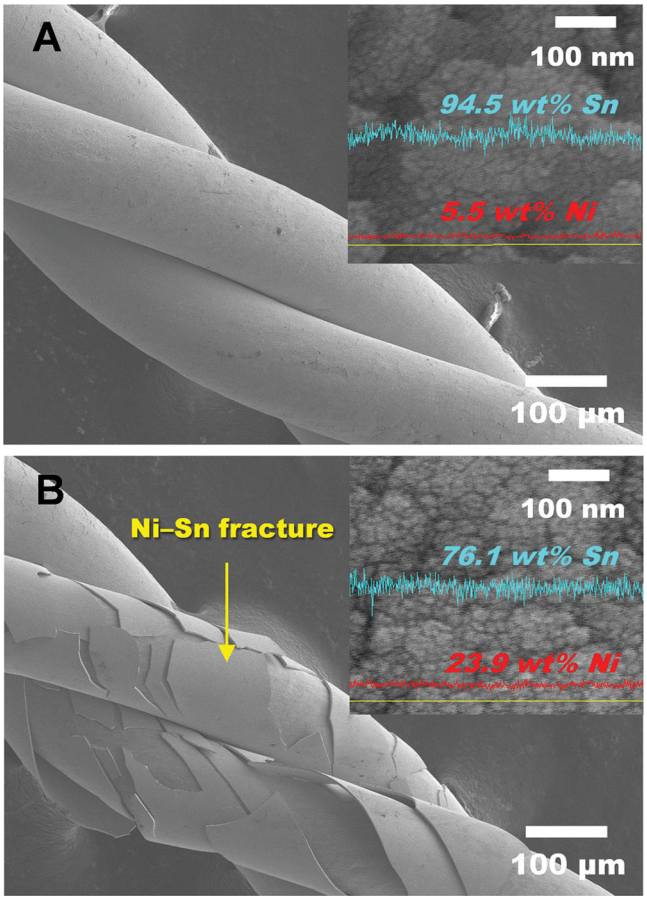

Figure 2. Scanning electron microscopy (SEM) images of a twisted bundle prepared with three strands of Ni-Sn-coated Cu wire. A) Low Ni content. B) High Ni content.

the liquid electrolyte for 1 day (Figure S3A, Supporting Information), followed by inserting it into the heat-shrinkable packaging insulator. To form the stable solid electrolyte interface (SEI) layer on the surface of the Ni-Sn anode, the prepared cable battery was charged and discharged between 4.2 and 2.5 V at the rate of 0.1C before proceeding with the cycling test.

Figures 4B and C show the charge and discharge performance of the cable batteries. The cable battery with the hollow anode reversibly charged and discharged with stable capacity retention close to its designed cell capacity (per unit length of cable battery) of 1 mAh cm^{-1}, showing a potential plateau at around 3.5 V. In contrast, the cable battery with the nonhollow anode showed much lower capacity and its capacity retention was also unstable. The inferior battery performance of the cable battery with the nonhollow anode possibly originates from its higher cell resistance: as shown in the impedance spectra of Figure 4D, both the Ohmic resistance (≈real impedance at 100 kHz) and the interfacial resistance (≈estimated diameter of the semicircle) of the cable battery with the hollow anode were much lower than those of the cable battery with the nonhollow anode. This strongly indicates that the electrolyte permeability/accessibility to the separator and active materials was much improved with the hollow anode (Figure S3 in the Supporting Information). Moreover, the hollow anode simplifies the manufacturing process, in that the electrolyte can be injected simply by inserting a needle into the hollow space within the anode (Figure 1A and Figure S3B). Therefore, our unique hollow-spiral (helical) anode architecture is the key design feature in terms of the realization of adequate cell performance and the simplicity of the manufacturing process.

The prerequisite for utilizing the cable battery as a flexible energy-storage device is adequate mechanical flexibility, which means that the battery should operate stably even under severe twisting and bending. For a conventional battery (that is, comprising a separator sandwiched between two electrodes using metal sheets as current collectors), it is known that strong external mechanical distortion leads to failure by three mechanisms: i) displacement of the component parts caused by motion relative to each other,[5] ii) crumbling of the electrode material and thus separation from the current collector,[4] and iii) the formation of short circuits when the sharp metal sheet penetrates the separator and allows contact between electrodes. These should be avoided in our design to attain reasonable mechanical flexibility. In order to prevent the active material from falling off and to suppress displacement of the components, heat-shrinkable tubing was used as the packaging insulator. It tightly fixes the cathode active material and the whole electrode assembly under large strain. In addition, the spring-like shape of the helical current collectors[7] (Cu and Al wires) allows them to undergo extreme deformation without leading to a short circuit.

Indeed, in our experiments, we found that our prototype was exceptionally flexible and could suffer large strain without malfunction. As shown in the photograph in **Figure 5**A, a prototype successfully operated a red LED screen and MP3 player (iPod shuffle fourth generation, Apple) under severe twisting and bending conditions (see Supporting Information, Movies S1 and S2), demonstrating its superior mechanical flexibility. To confirm how the mechanical stress actually affects the cable battery performance such as discharge characteristics, a mechanical bending test was performed by using a tensile tester (LF Plus, Lloyd Instruments) while measuring the closed circuit voltage of the cable battery (Figure 5B). This experiment was designed to see whether the cell voltage would be stably maintained during battery use in the case of external mechanical bending by the end user.

A battery was precharged to 4.0 V and fixed to the grips of a tensile tester. It was then continuously discharged at the rate of 0.1C while the grip distance was varied in the range from 7.5 to 1.0 cm. When the grips started to move after 20 min, the cell voltage slightly hopped ($\Delta V = 0.03$ V). However, aside from this initial bending-induced change, the cable battery showed stable discharge characteristics regardless of the degree of bending strain. Compared with other recent film-type flexible batteries,[4] the variation in the discharge characteristics of our battery is quite negligible, strongly indicating that our cable battery will exhibit mechanical robustness in real operating environments.

The stable electrochemical performance of our cable battery possibly results from its unique structural features, such as the helical electrode and current collectors, together with the choice of heat-shrinkable tubing as the packaging insulator. On the other hand, there was a slight loss of capacity after the mechanical bending of the cable battery. However, at present,

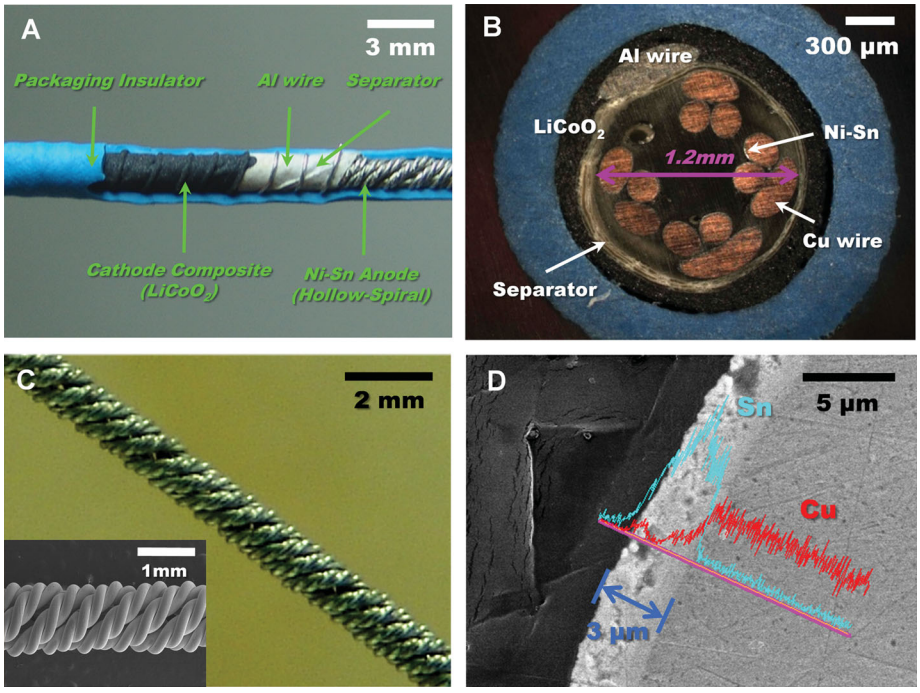

Figure 3. Components of the cable battery. A) Photograph showing side view of cable battery separated into component layers. B) Optical microscopy (OM) cross-sectional image of the cable battery with hollow anode having an outer diameter of 1.2 mm. C) Photograph and SEM image of the hollow-helix anode comprising 12 strands of Ni-Sn-coated Cu wire. D) SEM-EDS cross-sectional image of a Ni-Sn layer (thickness: ~3 μm) electrodeposited on the Cu wire (diameter: 150 μm).

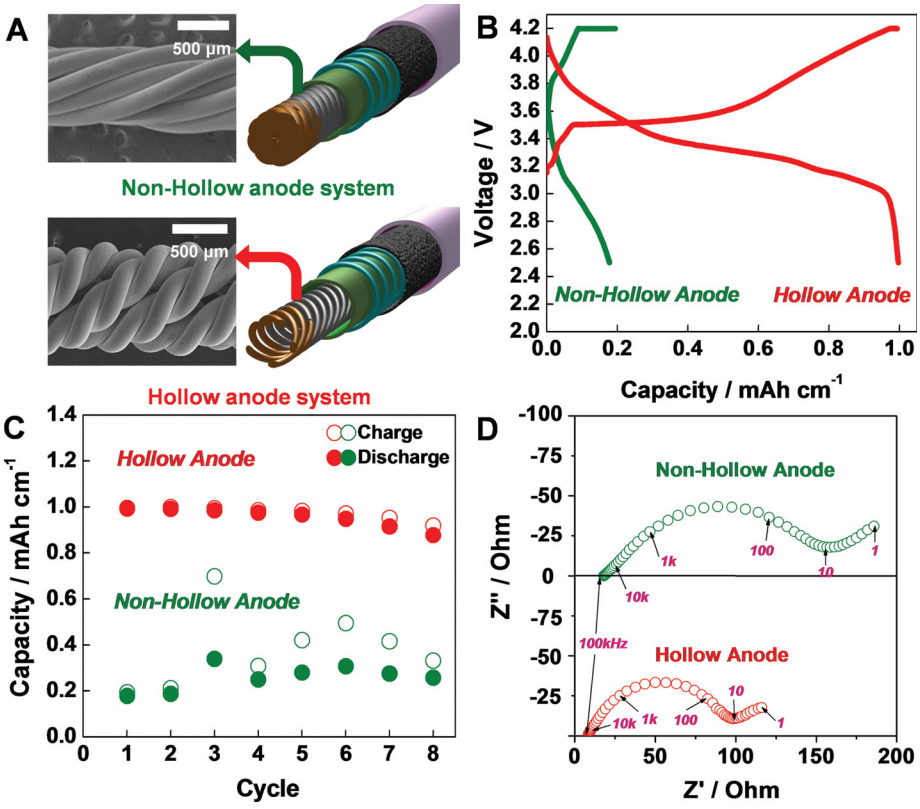

Figure 4. Electrochemical properties of the cable battery with hollow anode compared with a device with a nonhollow anode. A) Images of the cable batteries with nonhollow and hollow anode system. B) First charge and discharge profiles of cable batteries. C) Capacity retention of cable batteries. Cell capacity [mAh cm^{-1}] was defined as the capacity per unit length of the assembly before the metal (Al or Ni) tabs were connected. D) AC impedance spectra of cable battery after one cycle in the frequency range from 100 kHz to 1 Hz.

Adv. Mater. **2012**,
DOI: 10.1002/adma.201202196

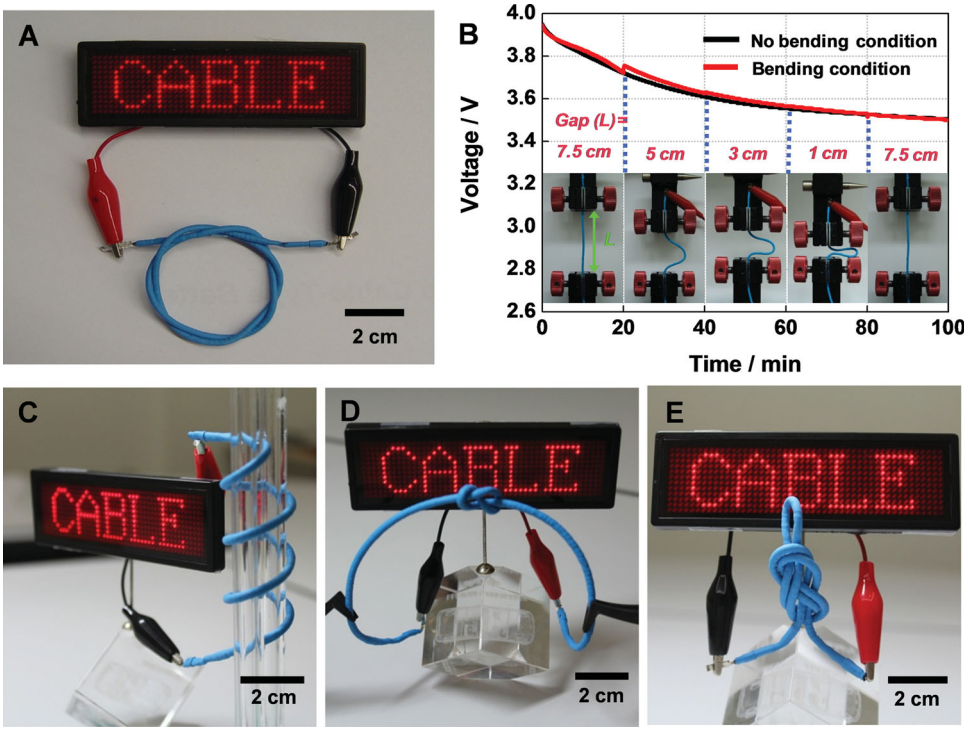

Figure 5. A) Photograph of the prototype cable battery of length 25 cm used to power a red LED screen. B) Discharge characteristics with variations in bending strain every 20 min. The discharge rate was 0.1C and the grip speed of the testing machine was 100 mm min^{-1}. C–E) Photographs of a highly flexible cable battery under various forms of bending and twisting. The cable battery exhibited stable operation even when bent.

it is not easy to say how much capacity is lost after bending, because the test standard for the mechanical stress of a cable battery has not been established. Mechanical test criteria/standards for the cable battery are being studied and the fatigue behavior and structural disintegration of the battery components (i.e., cathode, anode, separator, current collectors), together with the resulting degradation of electrochemical performance, are being investigated under the various types of cyclic stresses (bending/tying/compressing). Another important issue to be considered is the safety. No test criteria/standards for the safety of the cable battery are available at this time. The proper safety test criteria/standards should be established and the cable battery must meet all of the safety requirements before its market release. This would be another great challenge.

In summary, we have demonstrated that a cable-type battery with hollow-spiral, multiple-helix electrodes overcomes all the limitations of current flexible energy storage devices. The cable batteries suggested here can be connected/woven in parallel or in series, leading to battery units with a variety of shapes (including sheets) and energy and power densities. With further optimization of the battery components, the cable-type battery will undoubtedly have a great impact on the fields of portable, wearable, and flexible electronics in the near future.

Experimental Section

Electrochemical measurements: The capacities and cycle performances of the prepared cable batteries were examined by the following sequence: i) The cable battery was charged to 4.2 V at the rate of 0.1C (0.1 mA cm^{-1}) under constant current (CC) conditions and then maintained at a constant voltage (CV) of 4.2 V. CV charging was terminated when the current dropped below 0.05 mA cm^{-1}. ii) The cable battery was discharged to 2.5 V at the rate of 0.1C under CC conditions. The AC impedance measurements were conducted in the frequency range from 100 kHz to 1 Hz with a frequency response analyzer (Solartron 1255B) combined with an electrochemical interface (Solartron 1287).

Mechanical bending tests: A mechanical bending test was performed using a tensile tester (LF Plus, Lloyd Instruments) while measuring the voltage of the cable battery. After fixing the battery to the grips of a tensile tester, the battery was discharged from 4.0 V at the rate of 0.1C with variations in bending strain every 20 min. The grip speed and applied force of the testing machine were 100 mm min^{-1} and 14.0 N, respectively.

Supporting Information

Supporting Information is available from the Wiley Online Library or from the authors.

Acknowledgements

This work was supported by the Converging Research Center Program through the National Research Foundation of Korea funded by the Ministry of Education, Science and Technology (2012K001252).

Received: June 1, 2012
Revised: July 5, 2012
Published online:

[1] M. Armand, J. M. Tarascon, *Nature* **2008**, *451*, 652.
[2] J. M. Tarascon, M. Armand, *Nature* **2001**, *414*, 359.
[3] H. Nishide, K. Oyaizu, *Science* **2008**, *319*, 737.
[4] P. Hiralal, S. Imaizumi, H. E. Unalan, H. Matsumoto, M. Minagawa, M. Rouvala, A. Tanioka, G. A. J. Amaratunga, *ACS Nano* **2010**, *4*, 2730.
[5] C. Meng, C. Liu, L. Chen, C. Hu, S. Fan, *Nano Lett.* **2010**, *10*, 4025.
[6] L. Hu, M. Pasta, F. L. Mantia, L. Cui, S. Jeong, H. D. Deshazer, J. W. Choi, S. M. Han, Y. Cui, *Nano Lett.* **2010**, *10*, 708.
[7] J. Wang, C. Y. Wang, C.O. Too, G. G. Wallace, *J. Power Sources* **2006**, *161*, 1485.
[8] W. H. Meyer, *Adv. Mater.* **1998**, *10*, 439.
[9] B. Scrosati, *Nat. Nanotechnol.* **2007**, *2*, 598.
[10] J. Chen, Y. Liu, A. I. Minett, C. Lynam, J. Wang, G. G. Wallace, *Chem. Mater.* **2007**, *19*, 3595.
[11] A. Kiebele, G. Gruner, *Appl. Phys. Lett.* **2007**, *91*, 144104.
[12] J. S. Sakamoto, B. Dunn, *J. Electrochem. Soc.* **2002**, *149*, A26.
[13] K. T. Nam, D.-W. Kim, P. J. Yoo, C.-Y. Chiang, N. Meethong, P. T. Hammond, Y.-M. Chiang, A. M. Belcher, *Science* **2006**, *312*, 885.
[14] Y. J. Lee, H. Yi, W.-J. Kim, K. Kang, D. S. Yun, M. S. Strano, G. Ceder, A. M. Belcher, *Science* **2009**, *324*, 1051.
[15] X. Chen, K. Gerasopoulos, J. Guo, A. Brown, C. Wang, R. Ghodssi, J. N. Culver, *Adv. Funct. Mater.* **2011**, *21*, 380.
[16] M. Kotobuki, N. Okada, K. Kanamura, *Chem. Commun.* **2011**, *47*, 6144.
[17] A. M. Gaikwad, G. L. Whiting, D. A. Steingart, A. C. Arias, *Adv.Mater.* **2011**, *23*, 3251.
[18] J. W. Long, B. Dunn, D. R. Rolison, H. S. White, *Chem. Rev.* **2004**, *104*, 4463.
[19] M. D. Lima, S. Fang, X. Lepró, C. Lewis, R. Ovalle-Robles, J. Carretero-González, E. Castillo-Martínez, M. E. Kozlov, J. Oh, N. Rawat, C. S. Haines, M. H. Haque, V. Aare, S. Stoughton, A. A. Zakhidov, R. H. Baughman, *Science* **2011**, *331*, 51.
[20] H. Mukaibo, T. Sumi, T. Yokoshima, T. Momma, T. Osaka, *Electrochem. Solid-State Lett.* **2003**, *6*, A218.
[21] H. S. Jeong, J. H. Kim, S. Y. Lee, *J. Mater. Chem.* **2010**, *20*, 9180.

Adv. Mater. **2012**,
DOI: 10.1002/adma.201202196